Atomic-scale processes at the fluorite-water interface visualized by frequency modulation atomic force microscopy

Atomic-Scale Processes at Fluorite/Water Interface Visualized by Frequency Modulation Atomic Force Microscopy

Naritaka Kobayashi,[†,‡] Shiro Itakura,[†] Hitoshi Asakawa,[¶] and Takeshi Fukuma[*,†,¶,§]

Division of Electrical Engineering and Computer Science, Kanazawa University, Kakuma-machi, Kanazawa 920-1192, Japan, Japan Society for the Promotion of Science, Ichiban-cho, Chiyoda, Tokyo 102-8472, Japan, Bio-AFM Frontier Research Center, Kanazawa University, Kakuma-machi, Kanazawa 920-1192, Japan, and ACT-C, Japan Science and Technology Agency, Honcho 4-1-9, Kawaguchi 332-0012, Japan

E-mail: fukuma@staff.kanazawa-u.ac.jp

Phone: +81 76 234 4847. Fax: +81 76 234 4632

KEYWORDS: Calcium Fluoride, Crystal Growth, Dissolution, FM-AFM

[*]To whom correspondence should be addressed
[†]Division of Electrical Engineering and Computer Science, Kanazawa University
[‡]Japan Society for the Promotion of Science
[¶]Bio-AFM FRC, Kanazawa University
[§]ACT-C, JST

Atomic-Scale Processes at Fluorite/Water Interface Visualized by Frequency Modulation Atomic Force Microscopy

Abstract

The crystal growth and dissolution processes of a fluorite (CaF_2) crystal have attracted much attention due to the importance in the industrial, environmental and medical applications. While previous studies clarified nanoscale processes at fluorite/water interface, atomic-scale origins of the processes have yet to be understood. In this study, we have investigated atomic-scale processes at fluorite/water interface by frequency modulation atomic force microscopy (FM-AFM). We performed atomic-resolution imaging of a fluorite(111) surface in water (pH = 2 and 6.5), saturated solution (pH = 2 and 6) and supersaturated solution (pH = 6, σ = 10 and 100). Based on the results, we present three major findings. First, atomic-scale roughening of the crystal surface takes place at low pH due to the proton adsorption. Secondly, surface adsorbates with a subnanometer-scale height are formed on the crystal surface at high pH. They are most likely to be calcium hydroxo complexes physisorbed on the crystal surface. Finally, the formation of these complexes can be suppressed by increasing fluorite concentration owing to the increased proportion of Ca^{2+} and F^- in the electric double layer. These findings mark an important step towards the full understanding of the physicochemical processes at fluorite/water interface.

Keywords: Calcium Fluoride, Crystal Growth, Dissolution, FM-AFM

INTRODUCTION

Fluorite (CaF_2) crystals are widely used for various industrial applications. Examples include optical components for semiconductor lithography and other laser technologies[1,2] and scintillator for radioactivity investigations.[3,4] Thus, the crystal growth and dissolution processes of fluorite have intensively been studied to improve the crystal quality.[5,6] In addition, these processes play important roles in the formation of tooth enamel and pathogenesis of dental caries,[7,8] as well as in the desalination for oil and gas recovery[9–11] and water purification.[12–14] Therefore, the physicochemical processes taking place at fluorite/water interface are important in industrial, environmental and medical research fields.

Atomic force microscopy (AFM)[15] has a unique capability of imaging nanoscale structural changes at a solid/liquid interface. Thus, it has widely been used for investigating crystal growth and dissolution processes of various minerals. So far, Hillner *et al.* imaged crystal growth of a fluorite(111) surface in supersaturated solution by contact-mode AFM.[16] They reported the vertical growth of sharp asperities with a height of 10–500 nm on a flat terrace. Subsequently, Bosbach *et al.* imaged a fluorite(111) surface in an undersaturated solution by contact-mode AFM.[17] They found that the dissolution takes place by the formation of pits on terraces followed by the retreat of step edges. They also found the formation of nanoscale protrusions. Jordan *et al.* investigated the formation mechanism and the composition of the nanoscale protrusions by imaging fluorite(111) surface in various solutions with different pH.[18] Based on the results, they suggested that the protrusions correspond to multinuclear calcium (aquo) hydroxo complexes $[Ca_x(OH)_y^{2x-y}(aq)]$ connected to surface hydroxyl groups.

The previous research clarified nanoscale behavior of fluorite(111) surface in water such as the crystal growth and dissolution, and the formation of the protrusions. However, to understand the mechanism of these processes, we should also clarify atomic-scale interfacial phenomena such as adsorption or weak interaction of ions or other chemical species in the interfacial space with the crystal surface. Due to the limited resolution and the relatively large loading force of the conventional AFM, it has been difficult to visualize such delicate

atomic-scale interfacial phenomena.

Frequency modulation AFM (FM-AFM) has traditionally been used for atomic-scale investigations on various materials in vacuum.[19] However, recent advancement in instrumentation[20] has enabled its operation in liquid with true atomic resolution.[21] With this technique, we can perform reproducible atomic-scale imaging with a weak loading force (typically less than 100 pN). So far, this capability has mainly been employed for subnanometer-scale imaging of soft biological systems.[22–26] In contrast, it has hardly been utilized for investigating atomic-scale chemical processes at solid/liquid interfaces. For example, although the fluorite(111) surface is one of the most well-studied systems by FM-AFM in vacuum,[27–30] there have been no reports on experimental FM-AFM studies on the fluorite/water interface.

Another motivation for studying fluorite/water interface is to understand the imaging mechanism of liquid-environment FM-AFM. The imaging mechanism of fluorite(111) surface in vacuum has been extensively studied by the comparison between theory and experiment.[27–30] For example, two different contrasts in the atomic-scale images obtained by experiment were well reproduced by simulation. Based on the agreement, it was revealed that the contrast variation comes from the difference in the charge polarity of the tip front atom. This result is well known as one of the most successful examples of the AFM simulation study. Thus, the theoretical and technical bases for the AFM simulation of fluorite(111) surface are relatively well-prepared. In fact, Watkins *et al.* and Reischl *et al.* recently reported simulation of AFM measurements at a fluorite/water interface.[31–34] However, the lack of experimental results to be compared with those obtained by simulation has hindered the progress in understanding the imaging mechanism.

In this study, we have employed the atomic-resolution FM-AFM for directly visualizing atomic-scale interfacial phenomena taking place at fluorite/water interface. We performed FM-AFM imaging of a fluorite(111) surface in undersaturated, saturated and supersaturated solutions with different pH. Under these conditions, we expect that the surface shows different behaviors such as dissolution in undersaturated, equilibrium in saturated and growth in

supersaturated solutions. Based on the obtained results, we clarify the existence of various atomic-scale processes that have not been observed by conventional AFM. We also discuss mechanisms of the atomic-scale and nanoscale interfacial processes observed in this study.

EXPERIMENTAL METHODS

Fluorite(111) Surface

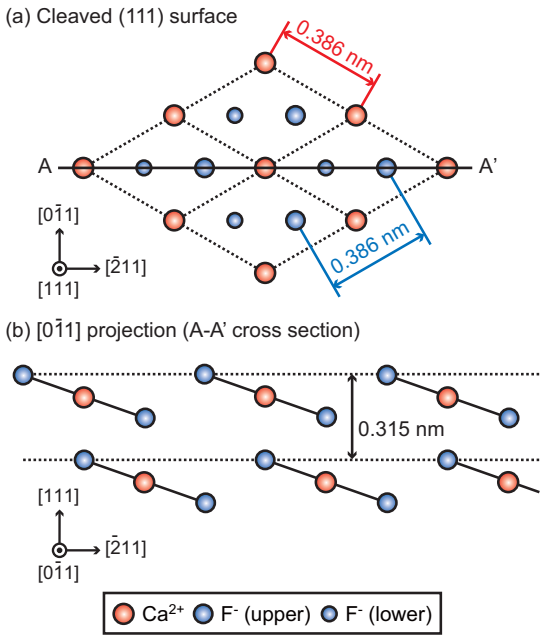

Figure 1: Schematic model of the crystal structure of fluorite. (a) Cleaved (111) surface. (b) [0$\bar{1}$1] projection.

Figure 1 shows an atomic-scale model of fluorite(111) surface. Fluorite crystal has a face-centered cubic (fcc) structure with a lattice constant of 0.546 nm. In the crystal, F^{-}-Ca^{2+}-F^{-} layers are stacked along the [111] direction with a spacing of 0.315 nm. Owing to the layered structure, we can easily cleave the crystal at an interface between the neighboring layers to obtain an atomically clean fluorite(111) surface. The topmost F^{-} and Ca^{2+} ions respectively form a hexagonal array with a spacing of 0.386 nm.

We used fluorite(111) substrate with a size of $2 \times 2 \times 1$ mm^3 (CFc101010S2, Ollie, Japan). The substrate was glued on a sample holder and cleaved with a razor blade. Immediately after the cleavage, 50 μl of solution was dropped onto the substrate. We performed FM-AFM imaging in the solution.

Solutions

The solutions used in this study include water (pH = 6.5 and 2), saturated solution (pH = 6 and 2) and supersaturated solution (pH = 6, σ = 10 and 100). σ is the degree of supersaturation defined by $\sigma = (c - c_{\mathrm{eq}})/c_{\mathrm{eq}}$, where c and c_{eq} denote the concentrations of the solution used for imaging and saturated solution, respectively. We prepared the solutions as follows. The solubility of fluorite is 1.51 mg/100 g-H_2O at 18°C and hence the saturated molar concentration of fluorite is 0.19 mM. We prepared 38 mM $CaCl_2$ solution and 76 mM KF solution. We mixed the same amount of these solutions and prepared supersaturated solution with $\sigma = 100$. The saturated and supersaturated ($\sigma = 10$) solutions were prepared by diluting this solution with pure water. We also prepared acidified solutions with pH = 2 by adding HCl. Note that c_{eq} of fluorite increases to 1.5 mM by decreasing pH to 2. Thus, we prepared the low pH solution by taking it into account.

FM-AFM Imaging

In this experiment, we used our home-built liquid-environment FM-AFM with an ultra-low-noise optical beam deflection sensor (< 10 fm/$\sqrt{\mathrm{Hz}}$).[21,35,36] A commercially available phase-locked loop (PLL) circuit (OC4, SPECS) is used for oscillating a cantilever at its resonance frequency (f_0) with constant amplitude (A) and for detecting the frequency shift (Δf) of the cantilever resonance induced by the tip-sample interaction force. All the images were obtained with constant Δf mode. The tip-sample distance is regulated by a commercially available AFM controller (RC4 and SC4, SPECS). We used a Si cantilever with Au backside coating (NCHAuD, Nanoworld). The typical f_0 in liquid and spring constant (k) are 150 kHz

and 42 N/m, respectively. The time indicated in the AFM images shown below corresponds to the time passed since the scan start. The time required for making the tip approach after the deposition of the solution on the cleaved crystal surface is typically 10 min.

RESULTS AND DISCUSSION

Surface Structure in Water (pH = 6.5)

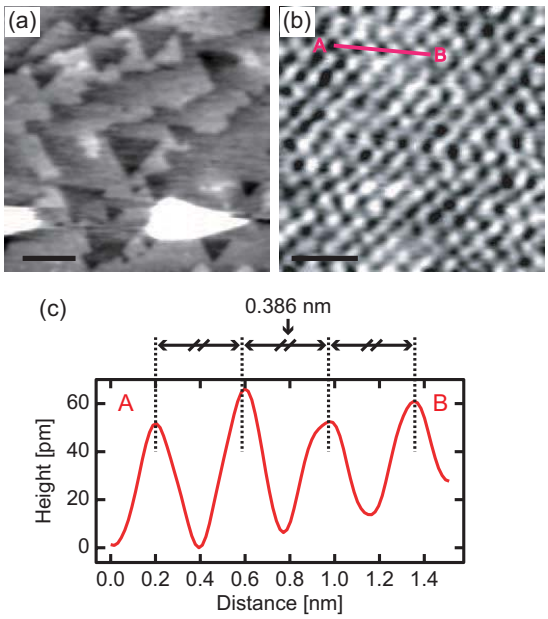

Figure 2: (a), (b) FM-AFM images of fluorite(111) surface taken in water (pH = 6.5). (a) $\Delta f = +122$ Hz. Scale bar = 100 nm. (b) $\Delta f = +1.89$ kHz. Scale bar = 1 nm. (c) Height profile measured along Line A-B indicated in (b).

Figure 2 shows FM-AFM images of a fluorite(111) surface obtained in water. The large-scale image (Figure 2(a)) shows steps and flat terraces. The step height corresponds to the thickness of a F^{-}-Ca^{2+}-F^{-} layer (0.315 nm). Figure 2(b) shows an FM-AFM image obtained on a terrace. The image shows hexagonally arranged atomic-scale contrast. The cross-sectional profile (Figure 2(c)) measured along Line A-B in Figure 2(b) reveals that the period of the surface corrugation agrees with the distance between the neighboring Ca^{2+}

or F^- ions (0.386 nm). Thus, the terrace initially exhibits an atomically clean structure without any adsorbates.

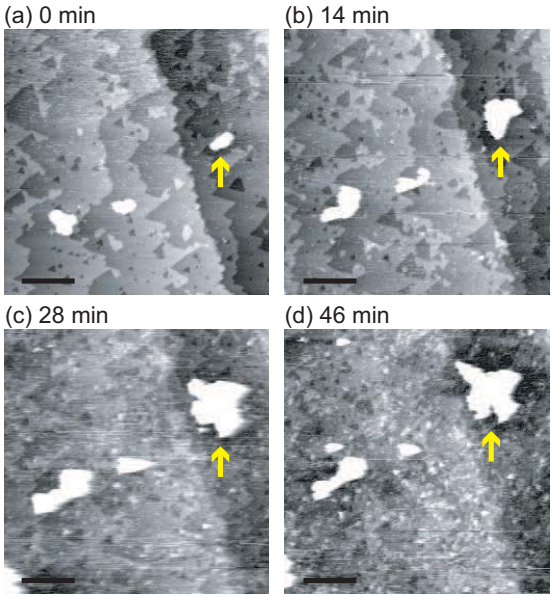

Figure 3: Successive FM-AFM images of fluorite(111) surface taken in water (pH = 6.5) at a fixed surface area (see also supplementary video). The images were taken at (a) 0 min, (b) 14 min, (c) 28 min and (d) 46 min after the scan start. $\Delta f = +122$ Hz. Scale bar = 100 nm. The arrows indicate the same but growing protrusion.

However, we found that such atomic-scale imaging cannot be performed for more than 30 min. Figure 3 shows successive FM-AFM images obtained at a fixed surface area. The images show that the triangular pits are formed on the terraces and laterally grow (see also supplementary video). The result confirms our expectation that the crystal surface should show dissolution in undersaturated solution. As time progresses, nanoscale protrusions with a constant height (2.8 ± 0.3 nm) are formed on the terraces and laterally grow (arrows in Figure 3). After 30 min, adsorbates with a height of 0.8 ± 0.3 nm and a lateral size of 13 ± 3 nm appear on the terraces.

In the previous AFM study, Jordan *et al.* reported the formation of similar structures to the nanoscale protrusions observed in our experiment.[18] According to their model, OH^- or water molecules near the surface interact with surface F^- vacancies to form surface hydroxyl

groups. The surface hydroxyl groups serve as ligands to bind Ca^{2+} and OH^- near the surface. The adsorbed ions further generate sorption sites for other ions in the interfacial space, leading to the continuous growth of the nanoscale protrusions. Based on this model, they suggested that the nanoscale protrusions consist of multinuclear calcium (aquo) hydroxo complexes. As this reaction should not progress in bulk fluorite solution, it takes place only in the electric double layer. Consequently, the protrusions have an almost uniform height (2.5–4 nm) and grow only in the lateral direction.

The proposed model is largely consistent with the results obtained in our experiments. The observed protrusions have an almost constant height (2.8 $\pm$ 0.3 nm). The measured height is within the previously reported range (2.5–4 nm). While the lateral size of the protrusions increases with time, the number of protrusions stays almost constant. This is also consistent with the model where the number of protrusions is determined by the number of surface F^- vacancies.

In this study, we were not able to find any atomic-scale defects that can be attributed to the surface F^- vacancies. This is probably because the F^- vacancies at the cleaved surface are already covered with the nanoscale protrusions by the time we start the atomic-scale AFM imaging. In fact, the number of nanoscale protrusions does not significantly increase after we start imaging. Under our experimental conditions, it takes more than 10 min to start atomic-scale imaging after the cleavage of the sample. Thus, the results indicate that the surface F^- vacancies, if they are responsible for nucleating the protrusions, may be maintained for less than 10 min.

Although we were not able to visualize atomic-scale dynamic processes around the surface F^- vacancies, such processes have been studied by theory[37] and experiments[38,39] in vacuum. The He diffraction study by Lehmann *et al.* suggested that water molecules dissociatively adsorb on the surface F^- vacancies to form the surface hydroxyl groups.[38] The molecular dynamics simulation by Foster *et al.* suggested that the energy barrier for the dissociative adsorption is relatively low compared to the case of other ionic crystal surfaces.[37] However,

their results also suggested that some of the water molecules can adsorb on the surface F^- vacancies without dissociation. More detailed understanding of such atomic-scale dynamic processes may be achieved when the operation speed of FM-AFM is improved in the future.

The surface adsorbates observed after 30 min from the scan start are most likely calcium hydroxo complexes not connected to the surface hydroxyl groups. Under this solution, the concentration of Ca^{2+} and OH^- near the interface is high enough to form the nanoscale protrusions. Thus, such calcium hydroxo complexes are likely to be formed in the interfacial space and deposited on the surface. In fact, this model can consistently explain all the results obtained in the following experiments.

Surface Structure in Acidified Water (pH = 2)

As the protrusions are formed by the reaction between surface hydroxyl groups and Ca^{2+} and OH^- near the surface, we should be able to suppress their formation by decreasing the concentration of OH^-, namely pH. In fact, Jordan *et al.* reported that the protrusions formed at the interface can be removed by replacing the solution with acidified water (pH = 2).[18] Based on this idea, we performed FM-AFM imaging in acidified water (pH = 2).

Figures 4(a)–4(c) show successive FM-AFM images obtained at a fixed surface area (see also supplementary video). The formation of protrusions was not observed for more than 1.5 h. The result confirms that the reduction of the pH is effective for suppressing the formation of protrusions. However, this does not prevent the surface dissolution and hence the step density gradually increases with time. In addition, the small-scale FM-AFM image taken on a terrace (Figure 4(d)) shows that the atomic-scale arrangement of the surface is not well-ordered. In the image, the areas indicated by the dotted lines show well-ordered atomic-scale structures while other areas appear to be disordered.

In the previous AFM study, Jordan *et al.* performed force curve measurements by static-mode AFM in a saturated fluorite solution and an acidified water on fluorite(111) surface.[18] They found that the curves taken in the saturated solution show strong adhesion force

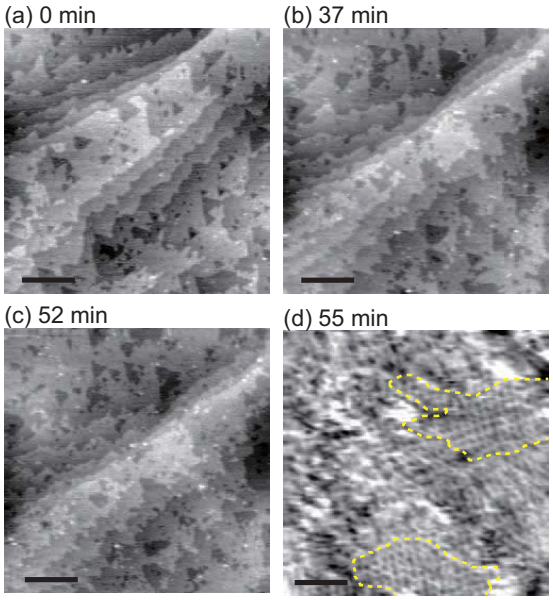

Figure 4: (a)-(c) Successive FM-AFM images of fluorite(111) surface taken in water (pH = 2) at a fixed surface area (see also supplementary video). The images were taken at (a) 0 min, (b) 37 min and (c) 52 min after the scan start. $\Delta f = +1.0$ kHz. Scale bar = 200 nm. (d) Small-scale FM-AFM image taken on a terrace. $\Delta f = +2.5$ kHz. Scale bar = 2 nm. The areas indicated by the dotted lines show well-ordered atomic-scale structure of the crystal surface.

while the ones obtained in the acidified water show long-range repulsive force. Based on these results and other previous studies, they suggested an increased proportion of H-bonds on fluorite(111) surface at lower pH. This previous report suggests that the atomic-scale roughening observed in our experiment could be caused by the proton adsorption.

In the meanwhile, one can also explain the atomic-scale roughening by partial dissolution of flat terraces. If the F^- ions constituting the surface are partially dissolved, the surface may appear to be corrugated. However, this model requires several assumptions that seem to be unlikely. First, the partial dissolution should create surface F^- vacancies that can serve as nucleation centers for nanoscale protrusions. However, we have not observed any formation of nanoscale protrusions. Secondly, if the dissolution takes place at the flat terrace, it should also take place at the step edges. However, our results show that the straight-shaped step edges do not show any changes for more than 90 min. Finally, the apparent height difference between the ordered and disordered areas (0.03–0.1 nm) is much lower than the single step height of the surface (0.315 nm). Note that the atomic-scale corrugation height measured by AFM is strongly influenced by the nature of the tip-sample interaction so that it does not necessarily represent the true geometrical surface corrugation. Nevertheless, it is unlikely that partially dissolved surface with irregularly arranged missing ions happens to be imaged as an atomically flat surface all over the terrace with apparent corrugation height of less than 0.1 nm. Due to these reasons, we consider that the observed atomic-scale roughening is most likely to be caused by the proton adsorption.

Surface Structure in Saturated Solution (pH = 6)

Figure 5 shows successive FM-AFM images obtained in saturated solution (pH = 6) at a fixed surface area (see also supplementary video). The first FM-AFM image obtained in this experiment (Figure 5(a)) shows flat terraces and straight steps with few kinks. The observed step arrangement was kept throughout the experiment (Figures 5(a)–5(e)). The triangular pits observed in undersaturated solution were not formed under these conditions. These

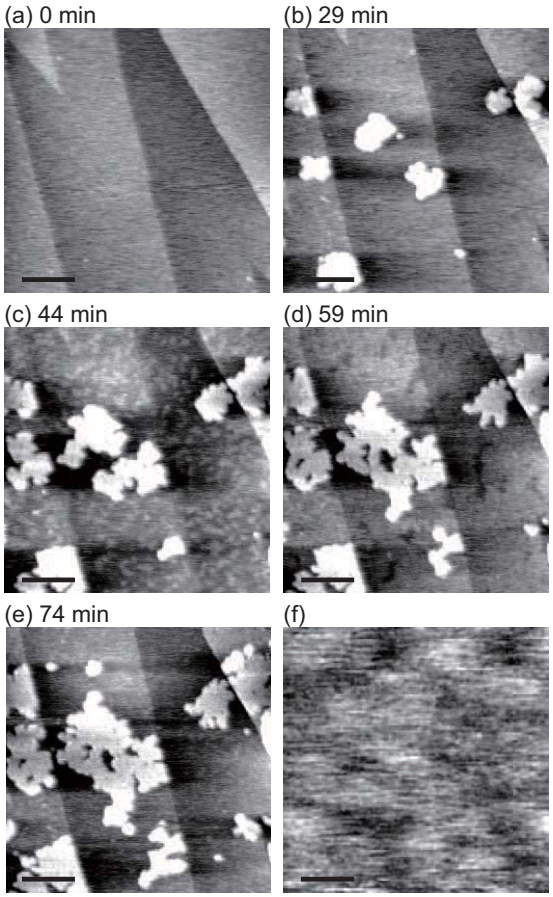

Figure 5: (a)-(e) Successive FM-AFM images of fluorite(111) surface taken in saturated solution (pH = 6) (see also supplementary video). The images were taken at (a) 0 min, (b) 29 min, (c) 44 min, (d) 59 min and (e) 74 min after the scan start. $\Delta f = +122$ Hz. Scale bar = 100 nm. (f) Small-scale FM-AFM image taken on a terrace. $\Delta f = +500$ Hz. Scale bar = 10 nm.

results confirm our expectation that no crystal growth or dissolution should take place in saturated solution.

As time progresses, nanoscale protrusions with a uniform height (1.25 ± 0.05 nm) are formed on the terraces and laterally grow. In the meantime, surface adsorbates with a height of 0.25–0.35 nm appear on the terraces (Figure 5(c)). They laterally grow too and eventually cover the whole surface (Figures 5(c)–5(e)). Although we imaged the surface of the adsorbates with a small scan size, we were not able to obtain any images showing atomic-scale contrasts (Figure 5(f)). We found that the protrusions are not always formed under these conditions while the surface adsorbates always appear on the terraces. We repeated a similar experiment seven times but the formation of protrusions was confirmed only three times.

As the structural features and behavior of the nanoscale protrusions are similar to those observed in water (Figure 3) and those reported by Jordan *et al.*,[18] we consider that they are also calcium hydroxo complexes connected to the surface hydroxyl groups. The poor reproducibility of the formation of the protrusions suggests that the increase of fluorite concentration may hinder the formation of the surface hydroxyl groups and hence the protrusions. The surface hydroxyl groups are formed by the reaction between OH^- or a water molecule and a surface F^- vacancy. If the concentration of fluorite is increased, the increased F^- near the surface may fill in the surface F^- vacancies and prevent their reaction with OH^- or water. In that case, subtle difference in the F^- concentration may result in significant difference in the formation of the protrusions, which may account for the observed poor reproducibility. This argument is further supported by the results obtained in supersaturated solutions.

The observed surface adsorbates have an apparent height of 0.25–0.35 nm, which is much higher than that of the atomically disordered structures observed in acidified water (Figure 4(d)). In addition, the small-scale FM-AFM images obtained on the adsorbates show no atomic-scale contrast (Figure 5(f)) while those obtained in acidified water show disordered

but atomic-scale contrast (Figure 4(d)). Thus, the surface adsorbates should be different from the atomically disordered structures observed in acidified water.

We consider that the observed surface adsorbates are calcium hydroxo complexes not connected to the surface hydroxyl groups. Similar to the water case, the formation of the protrusions suggests that the concentration of Ca^{2+} and OH^{-} is high enough to form calcium hydroxo complexes. In addition, the vague contrast observed in the small-scale FM-AFM image suggests that the surface adsorbates are not tightly bound to the surface and/or exhibit relatively large thermal fluctuations. This result is also consistent with our model where calcium hydroxo complexes formed in the interfacial space are physisorbed on the surface without chemical bond formation.

The height of the protrusions and that of the surface adsorbates is smaller than that in water. As previously reported,[18] the calcium hydroxo complexes are formed only in the electric double layer. The thickness of the electric double layer decreases with increasing the ionic strength. Thus, it is reasonable that the height of the protrusions and surface adsorbates are lower in saturated solution than that in water. This result also supports our interpretation that the surface adsorbates should consist of calcium hydroxo complexes.

Surface Structure in Acidified Saturated Solution (pH = 2)

Figures 6(a)–6(c) show successive large-scale FM-AFM images obtained in acidified saturated solution (pH = 2) at a fixed surface area (see also supplementary video). The images show flat terraces and straight steps with few kinks. In contrast to the case of the saturated solution with pH = 6, these features remain unchanged and the protrusions and surface adsorbates were not observed throughout the experiment ($>$ 1.5 h). These results confirm our expectation that the reduction of pH should suppress the formation of the protrusions and surface adsorbates.

Figures 6(d)–6(f) show successive small-scale FM-AFM images obtained at a fixed surface area. The images show atomic-scale but disordered contrasts. In the images, we found

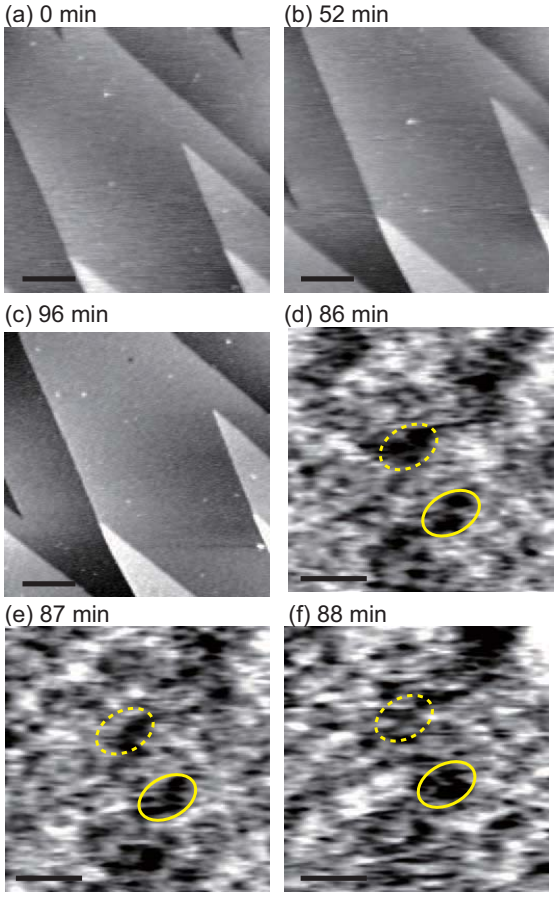

Figure 6: (a)-(c) Successive large-scale FM-AFM images of fluorite(111) surface taken in saturated solution (pH = 2) at a fixed surface area (see also supplementary video). The images were taken at (a) 0 min, (b) 52 min and (c) 96 min after the scan start. $\Delta f = +122$ Hz. Scale bar = 100 nm. (d)-(f) Successive small-scale FM-AFM images taken at a fixed surface area on a terrace. The images were taken at (a) 86 min, (b) 87 min and (c) 88 min after the scan start. $\Delta f = +1.46$ kHz. Scale bar = 2 nm.

that some features show time-dependent variation. While the area indicated by the solid line remains darker than the surrounding area, the other area indicated by the dotted line gradually becomes brighter (Figures 6(d)–6(f)). The apparent corrugation height of the disordered structure is less than 0.1 nm, which agrees with the apparent height of the similar structures observed in acidified water (Figure 4(d)). Such structure was not observed in the other solution with higher pH (∼6). From these results, we consider that the observed disordered structures are caused by the proton adsorption as discussed with the images shown in Figure 4(d).

With reducing pH, the concentration of protons should increase in the interfacial space. The protons in the interfacial space should not adsorb on the positively charged F^- vacancies. Instead, it is more likely that they coordinate around the negatively charged surface F^- ions. The observed contrast change suggests that the atomic-scale disordered structures should involve mobile species. Although we are not able to identify the species from the images, the possible species include the adsorbed protons, water molecules coordinating around the protons or surface ions. We do not think that the contrast change is induced by the tip scan. This is because forward and backward scan images of the disordered structure show almost the same contrast (see Figure S1 in Supporting Information).

However, the negative charge of the surface F^- should be largely compensated by the underlying Ca^{2+}. Thus, the binding force applied to the protons should be relatively small. In addition, water molecules around the surface F^- and the adsorbed protons may screen out the electrostatic interaction between these species and the surface.

Surface Structure in Supersaturated Solution (pH = 6, σ = 10)

Figures 7(a)–7(c) show successive large-scale FM-AFM images obtained in supersaturated solution (pH = 6, σ = 10) at a fixed surface area (see also supplementary video). The first image obtained in this experiment (Figure 7(a)) shows flat terraces and steps. While the steps observed in saturated solution (Figures 5(a) and 6(a)) appear to be straight, those

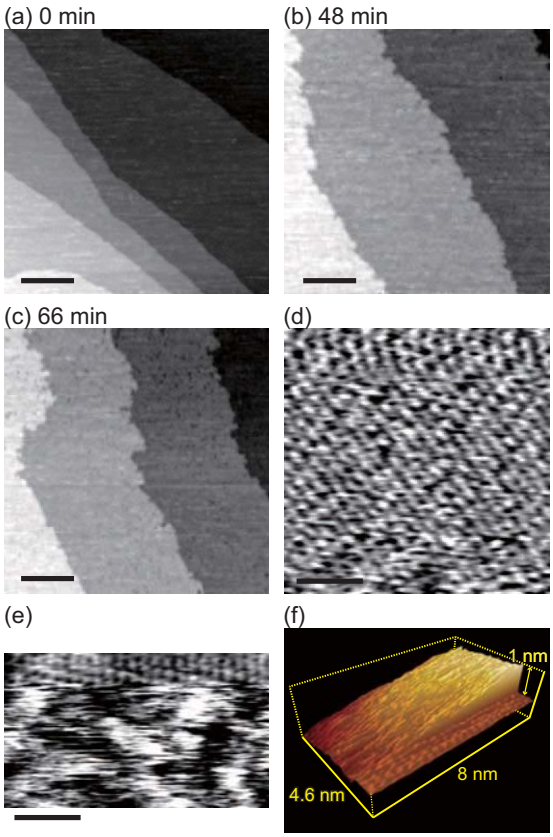

Figure 7: (a)-(c) Successive FM-AFM images of fluorite(111) surface taken in supersaturated solution (pH = 6, $\sigma = 10$) (see also supplementary video). The images were taken at (a) 0 min, (b) 48 min and (c) 66 min after the scan start. $\Delta f = +500$ Hz. Scale bar = 100 nm. (d)-(f) Small-scale images taken on a terrace. (d) $\Delta f = +2.5$ kHz. Scale bar = 1.5 nm. (e), (f) $\Delta f = +1.0$ kHz. Scale bar = 2 nm. Note that the same data is shown in (e) line-by-line flattened and (f) 3D views.

observed in this solution are curved. The flat terraces show lateral growth from the step edges (Figures 7(a)–7(c)). The growth rate is initially fast but gradually decays to a constant value of ∼22 nm/min. We found that the newly created terraces have more nanoscale depressions than the original ones. In addition, the steps become more corrugated due to the increase of kinks. Such increase of the number of kinks and depressions suggests that the surface structure does not reach its thermodynamic equilibrium due to the fast crystal growth.

The formation of protrusions was not observed throughout the experiment (> 1 h). This result confirms our expectation that the increase of the fluorite concentration can suppress the formation of protrusions. According to the previous study,[18] calcium hydroxo complexes are formed only in the electric double layer. With increasing the fluorite concentration, the proportion of Ca^{2+} and F^- in the electric double layer should increase and that of H^+ and OH^- should decrease. Consequently, the possibility of the reaction between Ca^{2+} and OH^- in the electric double layer may be reduced.

On the flat terraces, we were able to obtain atomic-scale FM-AFM images as shown in Figure 7(d). However, the obtained atomic-scale contrasts are blurred and individual atoms are not clearly resolved. In addition, the image contrast often shows discontinuous changes as shown in Figure 7(e). Thus, we found it difficult to complete a single frame scan without instability. Although such instability is often explained by the atomic-scale tip change, this is not the case in this particular experiment. If the contrast change was caused by the tip change, the image height would be changed by a fixed amount. However, the three-dimensional view (Figure 7(f)) of the image shown in Figure 7(e) reveals that the height change is not uniform. Such a height change cannot be explained by a tip change.

The observed instability can be explained by the adsorption and desorption of the calcium hydroxo complexes weakly interacting with the surface. If a calcium hydroxo complex is adsorbed on the surface during the tip scan, it should cause a sudden increase of the tip height but the increase is unlikely to be uniform. Similarly, sudden drops of the tip height, which were also often observed during the experiment, can be explained by desorption of the

calcium hydroxo complexes. Furthermore, this model can consistently explain the blurred atomic-scale contrasts. If the surface is covered with calcium hydroxo complexes, the tip has to push them away to reach the crystal surface. Thus, a relatively high loading force is required for atomic-resolution imaging. Such a high loading force often leads to a blurred atomic-scale contrast due to the displacement of surface or tip atoms and the increase of the effective interaction area.

Although we have attributed both the nanoscale protrusions (figures 3 and 5) and surface adsorbates (figure 7) to calcium hydroxo complexes, they have different structural features and show different behaviors. While the nanoscale protrusions have a constant height, the height of the surface adsorbates is not uniform, as shown in figure 7(f). While we have not seen any displacement of the nanoscale protrusions caused by the tip scan, the surface adsorbates are easily removed by the tip. Such difference suggests that the nanoscale protrusions are more tightly bound to the surface than the surface adsorbates. This is consistent with our interpretation that the nanoscale protrusions are connected to the surface hydroxyl groups while the surface adsorbates are weakly physisorbed on the surface.

In the supersaturated solution, the concentration of F^- ions in the interfacial space should be higher than that in undersaturated or saturated solutions. Thus, some of the surface F^- vacancies should be filled with F^- ions in the interfacial space. The absence of the surface F^- vacancies should prevent the formation of the surface hydroxyl groups and hence the nanoscale protrusions. In contrast, the surface adsorbates are formed in the interfacial space and subsequently physisorbed on the surface. This process does not involve the surface hydroxyl groups. Therefore, the surface adsorbates can be created even when the formation of the nanoscale protrusions is prevented.

Surface Structure in Supersaturated Solution (pH = 6, σ = 100)

Figures 8(a)–8(d) show the successive FM-AFM images obtained at a fixed surface area (see also supplementary video). The images show flat terraces and corrugated steps. The

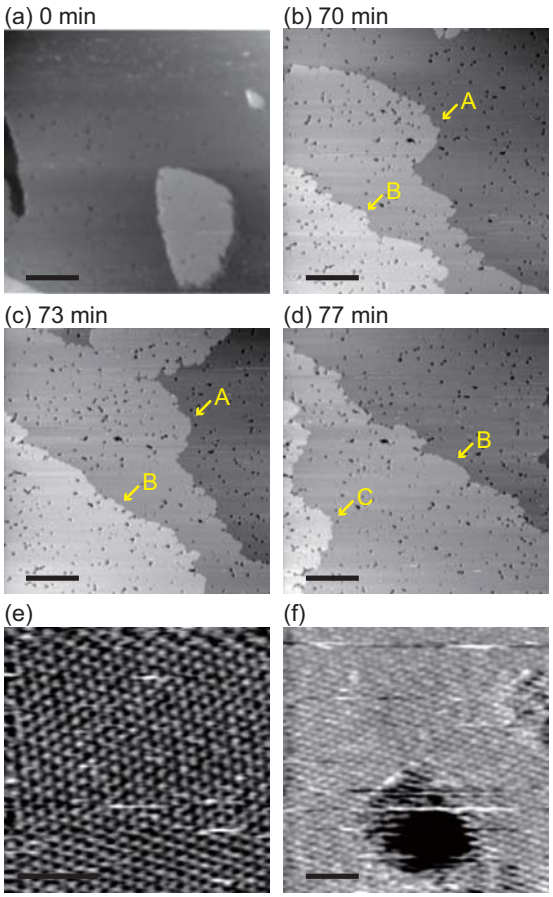

Figure 8: (a)-(d) Successive FM-AFM images of fluorite(111) surface taken in supersaturated solution (pH = 6, $\sigma = 100$) (see also supplementary video). The images were taken at (a) 0 min, (b) 70 min (c) 73 min and (c) 77 min after the scan start. $\Delta f = +500$ Hz. Scale bar = 100 nm. The arrows with the same label indicate the same step. (e), (f) Small-scale FM-AFM images taken on a terrace. $\Delta f = +2.0$ kHz. Scale bar = 3 nm.

terraces show lateral growth, as indicated by Arrows A–C. The growth rate is initially fast but decays to a constant value of ∼34 nm/min. These structural features and behavior are mostly similar to those observed with $\sigma = 10$. However, the growth rate at the steady state is faster owing to the increased σ. This is probably the reason for the increase of the nanoscale depressions on the terraces.

Under specific experimental conditions, surface adsorbates can be imaged as depressions in AFM images. However, we have not seen any displacement of the depressions at the terraces during the experiments. Considering the large scan size and fast scan speed, it is unlikely that nanoscale clusters adsorbed on the surface are not displaced by the tip scan. Therefore, we consider that the observed depressions should indeed correspond to pits rather than adsorbates.

On the terraces, we were able to obtain atomic-resolution images. For example, the image in Figure 8(e) shows hexagonal arrangement of the atoms constituting the fluorite(111) surface. Such an atomic-scale arrangement can be imaged even at the edge of the nanoscale depressions (Figure 8(f)). Although the multiple steps observed at the upper left edge of the nanoscale depression appear to be a tip artifact, the other part of the edge shows an atomically sharp structure. Compared to the case with $\sigma = 10$, we found that the imaging conditions are more stable and the obtained atomic-scale contrasts are clearer.

At this stage, we are not able to determine if the atomic-scale protrusions correspond to the surface atoms or hydration structures. Detailed understanding of the atomic-scale contrasts generally requires comparison between theory and experiment. Although this is beyond the scope of the present work, the establishment of the atomic-scale imaging conditions achieved in this study should enable such detailed studies on the imaging mechanism in the near future.

The formation of protrusions or surface adsorbates was not observed throughout the experiments ($>$ 1 h). In addition, the discontinuous contrast changes (e.g. Figure 7(e)) caused by the adsorption or desorption of the surface adsorbates were not observed. These

results suggest that the increased proportion of Ca^{2+} and F^- in the electric double layer can almost completely suppress the formation of the calcium hydroxo complexes.

CONCLUSIONS

Table 1: Summary of the interfacial phenomena observed in various aqueous solutions.

	Crystal Growth	Protrusions	Adsorbates	Protons
Water (pH: 6.5)	Dissolution	Yes	Yes	No
Acidified water (pH: 2)	Dissolution	No	No	Yes
Saturated (pH: 6)	Equilibrium	Yes	Yes	No
Acidified Saturated (pH: 2)	Equilibrium	No	No	Yes
Supersaturated (pH: 6, σ: 10)	Growth	No	Yes	No
Supersaturated (pH: 6, σ: 100)	Growth	No	No	No

In this study, we have investigated atomic-scale processes taking place at fluorite/water interface. We performed FM-AFM imaging of the fluorite(111) surface in various solutions including water (pH = 2 and 6.5), saturated solution (pH = 2 and 6) and supersaturated solution (pH = 6, σ = 10 and 100). The interfacial phenomena observed in this study are summarized in Table 1. By analyzing the results, we have presented the following three major findings.

First, we found that the atomic-scale surface roughening takes place at low pH probably due to the proton adsorption as shown in Figures 4(d) and 6(d)–6(c). In the previous report, the increase of H-bonds on fluorite(111) surface has been suggested based on the results obtained by the force curve measurements.[18] The atomic-scale images obtained in this study further strengthened this idea and provided a real-space description of this interfacial phenomenon.

Secondly, we found the existence of the surface adsorbates at high pH as shown in Figures 3(d), 4(c)–4(f) and 7(e)–7(f). Based on their behavior, we consider that they are most likely to be calcium hydroxo complexes. Unlike the nanoscale protrusions reported so far, the lateral distribution of the surface adsorbates is not limited to the vicinity of the F^-

vacancies. This is because they are not connected to the surface hydroxyl groups but weakly interact with the fluorite surface. In fact, we confirmed that they can be removed by the tip in saturated solution with $\sigma = 10$ (Figures 7(e)–7(f)).

Finally, we found that the increase of fluorite concentration in solution can prevent the formation of the calcium hydroxo complexes, as shown in Figures 7 and 8. The increase of the fluorite concentration results in the increase of Ca^{2+} and F^- and the decrease of OH^- concentrations in the electric double layer. Consequently, the formation of the calcium hydroxo complexes are suppressed. In addition, we suggest that the increased concentration of F^- ions in the electric double layer fills in the surface F^- vacancies, which prevents the formation of the surface hydroxyl groups and hence the nanoscale protrusions.

These findings improve our understanding of the interfacial phenomena taking place at the fluorite/water interface. So far, such an atomic-scale study of the interfacial phenomena has been hindered by the limited performance of the conventional AFM. Owing to the high spatial resolution and the small loading force of FM-AFM, we were able to directly visualize atomic-scale interfacial phenomena. This capability should also be useful in other studies on various interfacial phenomena such as crystal growth and dissolution, catalytic reactions and corrosion processes. Therefore, the results obtained here should stimulate the future applications of FM-AFM to the studies in physical chemistry.

Acknowledgement

The authors are grateful to Alexander Shluger and Matthew Watkins for valuable and stimulating discussions. This work was supported by ACT-C, Japan Science and Technology Agency.

Supporting Information Available

A figure showing forward and backward scan images of the atomically-disordered surface structure. Video files consisting of successive FM-AFM images of CaF2(111) surface obtained

in water, acidified water, saturated solution, acidified saturated solution, supersaturated solution with $\sigma = 10$ and supersaturated solution with $\sigma = 100$.

This material is available free of charge via the Internet at `http://pubs.acs.org/`.

References

(1) Senguttuvan, N.; Aoshima, M.; Sumiya, K.; Ishibashi, H. Oriented Growth of Large Size Calcium Fluoride Single Crystals for Optical Lithography. *J. Cryst. Growth* **2005**, *280*, 462–466.

(2) Nicoara, I.; Stef, M.; Pruna, A. Growth of YbF_3-Doped CaF_2 Crystals and Characterization of Yb^{3+}/Yb^{2+} Conversion. *J. Cryst. Growth* **2008**, *310*, 1470–1475.

(3) Wakahara, S.; Furuya, Y.; Yanagida, T.; Yokota, Y.; Pejchal, J.; Sugiyama, M.; Kawaguchi, N.; Totsuka, D.; Yoshikawa, A. Crystal Growth and Scintillation Properties of Ce-Doped Sodium Calcium Lutetium Complex Fluoride. *Opt. Mater.* **2012**, *34*, 729–732.

(4) Zhang, Y.; Xiang, X.; Weber, W. J. Scintillation Response of CaF_2 to H and He over A Continuous Energy Range. *Nucl. Instr. and Meth.* **2008**, *266*, 2750–2753.

(5) Perez, L. A.; Nancollas, G. H. Kinetics of Crystallization and Flocculation of Calcium Fluoride. *Coll. Surf.* **1991**, *52*, 231–240.

(6) Moller, H.; Madsen, H. E. L. Growth Kinetics of Calcium Fluoride in Solution. *J. Cryst. Growth* **1985**, *71*, 673–681.

(7) Aoba, T.; Fejerskov, O. Dental Fluorosis: Chemistry and Biology. *Crit. Rev. Oral Biol. Med.* **2002**, *13*, 155–170.

(8) Prymak, O.; Sokolova, V.; Peitsch, T.; Epple, M. The Crystallization of Fluoroapatite Dumbbells from Supersaturated Aqueous Solution. *Cryst. Growth Des.* **2006**, *6*, 498–506.

(9) Hamza, S. M.; Hamdona, S. K. Kinetics of Dissolution of Calcium Fluoride Crystals in Sodium Chloride Solutions: Influence of Additives. *J. Phys. Chem.* **1991**, *95*, 3149–3152.

(10) Amjad, Z. Performance of Inhibitors in Calcium Fluoride Crystal Growth Inhibition. *Langmuir* **1993**, *9*, 597–600.

(11) de Vreugd, C. H.; ter Horst, J. H.; Durville, P. F. M.; Witkamp, G. J.; van Rosmalen, G. M. Adsorption Behaviour of Polyelectrolytes on Calcium Fluoride: Part I: Influence of The pH and The Ionic Strength on The Adsorption Isotherms. *Coll. Surf. A* **1999**, *154*, 259–271.

(12) Tai, C. Y. Crystal Growth Kinetics of Two-Step Growth Process in Liquid Fluidized-Bed Crystallizers. *J. Cryst. Growth* **1999**, *206*, 109–118.

(13) Tai, C. Y.; P. C, . C.; Tsao, T. M. Growth Kinetics of CaF_2 in A pH-Stat Fluidized-Bed Crystallizer. *J. Cryst. Growth* **2006**, *290*, 576–584.

(14) Eksteen, J. J.; Pelser, M.; Onyango, M. S.; Lorenzen, L.; Aldrich, C.; Georgalli, G. A. Effects of Residence Time and Mixing Regimes on The Precipitation Characteristics of CaF_2 and MgF_2 from High Ionic Strength Sulphate Solutions. *Hydrometallurgy* **2008**, *91*, 104–112.

(15) Binnig, G.; Quate, C. F.; Gerber, C. Atomic Force Microscope. *Phys. Rev. Lett.* **1986**, *56*, 930–933.

(16) Hillner, P. E.; Manne, S.; Hansma, P. K.; Gratz, A. J. Atomic Force Microscope: A New Tool for Imaging Crystal Growth Processes. *Faraday Discuss.* **1993**, *95*, 191–197.

(17) Bosbach, D.; Jordan, G.; Rammensee, W. Crystal Growth and Dissolution Kinetics of Gypsum and Fluorite: An in Situ Scanning Force Microscope Study. *Eur. J. Mineral.* **1995**, *7*, 267–276.

(18) Jordan, G.; Rammensee, W. Growth and Dissolution on The CaF_2(111) Surface Observed by Scanning Force Microscopy. *Surf. Sci.* **1997**, *371*, 371–380.

(19) Morita, S., Wiesendanger, R., Meyer, E., Eds. *Noncontact Atomic Force Microscopy (Nanoscience and Technology)*; Springer Verlag, 2002.

(20) Fukuma, T.; Kimura, M.; Kobayashi, K.; Matsushige, K.; Yamada, H. Development of Low Noise Cantilever Deflection Sensor for Multienvironment Frequency-Modulation Atomic Force Microscopy. *Rev. Sci. Instrum.* **2005**, *76*, 053704.

(21) Fukuma, T.; Kobayashi, K.; Matsushige, K.; Yamada, H. True Atomic Resolution in Liquid by Frequency-Modulation Atomic Force Microscopy. *Appl. Phys. Lett.* **2005**, *87*, 034101.

(22) Hoogenboom, B. W.; Hug, H. J.; Pellmont, Y.; Martin, S.; Frederix, P. L. T. M.; Fotiadis, D.; Engel, A. Quantitative Dynamic-Mode Scanning Force Microscopy in Liquid. *Appl. Phys. Lett.* **2006**, *88*, 193109.

(23) Higgins, M.; Polcik, M.; Fukuma, T.; Sader, J.; Nakayama, Y.; Jarvis, S. P. Structured Water Layers Adjacent to Biological Membranes. *Biophys. J.* **2006**, *91*, 2532–2542.

(24) Yamada, H.; Kobayashi, K.; Fukuma, T.; Hirata, Y.; Kajita, T.; Matsushige, K. Molecular Resolution Imaging of Protein Molecules in Liquid Using Frequency Modulation Atomic Force Microscopy,.

(25) Asakawa, H.; Fukuma, T. The Molecular-Scale Arrangement and Mechanical Strength of Phospholipid/Cholesterol Mixed Bilayers Investigated by Frequency Modulation Atomic Force Microscopy in Liquid. *Nanotechnology* **2009**, *20*, 264008.

(26) Nagashima, K.; Abe, M.; Morita, S.; Oyabu, N.; Kobayashi, K.; Yamada, H.; Ohta, M.; Kokawa, R.; Murai, R.; Matsumura, H.; *et al.*, Molecular Resolution Investigation of

Tetragonal Lysozyme (110) Face in Liquid by Frequency-Modulation Atomic Force Microscopy. *J. Vac. Sci. Technol. B* **2010**, *28*, C4C11.

(27) Foster, A. S.; Barth, C.; Shluger, A. L.; Reichling, M. Unambiguous Interpretation of Atomically Resolved Force Microscopy Images of an Insulator. *Phys. Rev. Lett.* **2001**, *86*, 2373–2376.

(28) Foster, A. S.; Shluger, A. L.; Nieminen, R. M. Quantitative Modelling in Scanning Force Microscopy on Insulators. *Appl. Surf. Sci.* **2002**, *188*, 306–318.

(29) Foster, A. S.; Barth, C.; Shluger, A. L.; Nieminen, R. M.; Reichling, M. Role of Tip Structure and Surface Relaxation in Atomic Resolution Dynamic Force Microscopy: CaF_2(111) as A Reference Surface. *Phys. Rev. B* **2002**, *66*, 235417.

(30) Foster, A. S.; Shluger, A. L.; Nieminen, R. M. Realistic Model Tips in Simulations of nc-AFM. *Nanotechnology* **2004**, *15*, S60–S64.

(31) Watkins, M.; Shluger, A. L. Mechanism of Contrast Formation in Atomic Force Microscopy in Water. *Phys. Rev. Lett.* **2010**, *105*, 196101.

(32) Reischl, B.; Watkins, M.; S.Foster, A. Free Energy Approaches for Modeling Atomic Force Microscopy in Liquids. *J. Chem. Theory Comput.* **2012**, *9*, 600–608.

(33) Watkins, M.; Reischl, B. A Simple Approximation for Forces Exerted on An AFM Tip in Liquid. *J. Chem. Phys.* **2013**, *138*, 154703.

(34) Watkins, M.; Berkowitz, M. L.; Shluger, A. L. Role of Water in Atomic Resolution AFM in Solutions. *Phys. Chem. Chem. Phys.* **2013**, *13*, 12584–12594.

(35) Fukuma, T.; Jarvis, S. P. Development of Liquid-Environment Frequency Modulation Atomic Force Microscope with Low Noise Deflection Sensor for Cantilevers of Various Dimensions. *Rev. Sci. Instrum.* **2006**, *77*, 043701.

(36) Fukuma, T. Wideband Low-Noise Optical Beam Deflection Sensor with Photothermal Excitation for Liquid-Environment Atomic Force Microscopy. *Rev. Sci. Instrum.* **2009**, *80*, 023707.

(37) Foster, A. S.; Trevethan, T.; Shluger, A. L. Structure and Diffusion of Intrinsic Defects, Adsorbed Hydrogen, and Water Molecules at The Surface of Alkali-Earth Fluorides Calculated Using Density Functional Theory. *Phys. Rev. B* **2009**, *80*, 115421.

(38) Lehmann, A.; König, G.; Rieder, K. H. He-Diffraction Study of Defect Correlated Water Adsorption on The CaF_2 (111) Surface. *Chem. Phys. Lett.* **1995**, *235*, 65–68.

(39) Wu, Y.; Mayer, J. T.; Garfunkel, E.; Madey, T. E. X-ray Photoelectron Spectroscopy Study of Water Adsorption on BaF_2(111) and CaF_2(111) Surfaces. *Langmuir* **1994**, *10*, 1482–1487.

Graphical TOC Entry